

## Supplementary Information

# **Boron-Nitride Based Dispersive Composite Coating on Nickel-Rich Layered Cathode for Enhanced Cycle Stability and Safety**

Hsi Chen<sup>1,3</sup>, Yan-Cheng Chen<sup>1</sup>, Hao-Wen Liu<sup>1</sup>, Shu-Jui Chang<sup>1</sup>, Cheng-Hung Liao<sup>1</sup>,  
Senthil-Kumar Parthasarathi<sup>1</sup>, Satish Bolloju<sup>1</sup>, Yu-Ting Weng<sup>1</sup>, Jyh-Fu Lee<sup>2</sup>, Jin-Ming  
Chen<sup>2</sup>, Hwo-Shuenn Sheu<sup>2</sup>, Chih-Wen Pao<sup>2</sup>, and Nae-Lih Wu<sup>1,3,\*</sup>

<sup>1</sup>*Department of Chemical Engineering, National Taiwan University, Taipei 10617, Taiwan.*

<sup>2</sup>*National Synchrotron Radiation Research Center, Hsinchu 30076, Taiwan.*

<sup>3</sup>*Advanced Research Center for Green Materials Science and Technology, National Taiwan University, Taipei, 106, Taiwan.*

---

\*To whom correspondence should be addressed: [nlw001@ntu.edu.tw](mailto:nlw001@ntu.edu.tw)

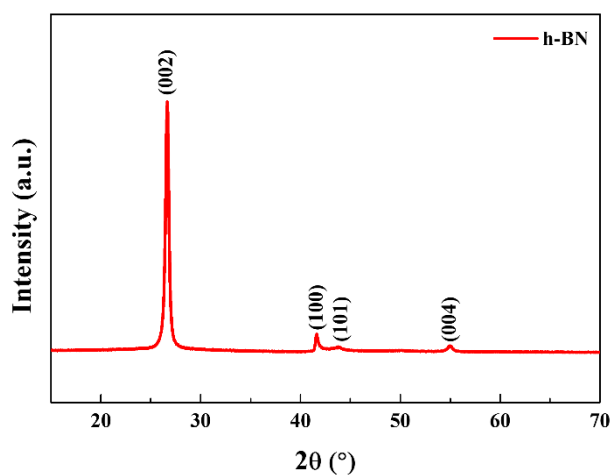


**Figure S1.** XRD pattern of h-BN.

**Table S1.** Rietveld refinement results of pristine NCM.

Sample	NCM				
Rwp (%)	1.39				
a (Å)	2.87157				
c (Å)	14.19595				
c/a	4.94362				
Volume (Å <sup>3</sup> )	101.375				
Atom	Site	x	y	z	Occupancy
Mn	3a	0	0	0	0.05
Co					0.12
Ni					0.819
Li					0.0111(4)
Li	3b	0	0	1/2	0.989
Ni					0.0111(4)
O	6c	0	0	0.25700(4)	1

**Table S2.** Rietveld refinement results of NCM@PB.

Sample	NCM@PB				
Rwp (%)	1.49				
a (Å)	2.87199				
c (Å)	14.19788				
c/a	4.94357				
Volume (Å <sup>3</sup> )	101.419				
Atom	Site	x	y	z	Occupancy
Mn	3a	0	0	0	0.05
Co					0.12
Ni					0.819
Li					0.0105(5)
Li	3b	0	0	1/2	0.989
Ni					0.0105(5)
O	6c	0	0	0.25757(4)	1

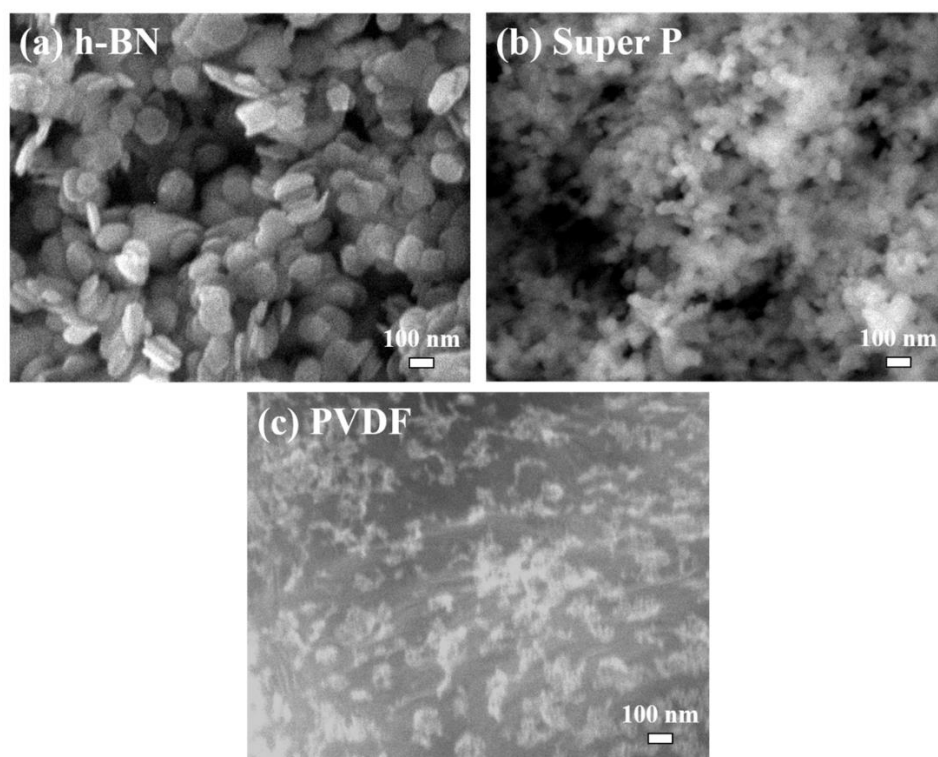


**Figure S2.** SEM images of (a) h-BN, (b) Super P and (c) calcined PVDF.

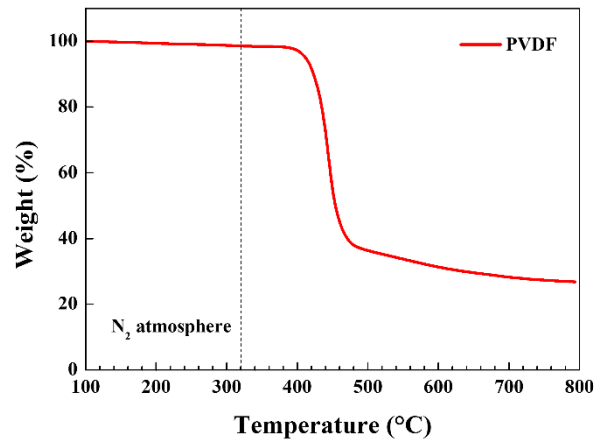


Figure S3. TGA curve of PVDF under N<sub>2</sub>-atmosphere.

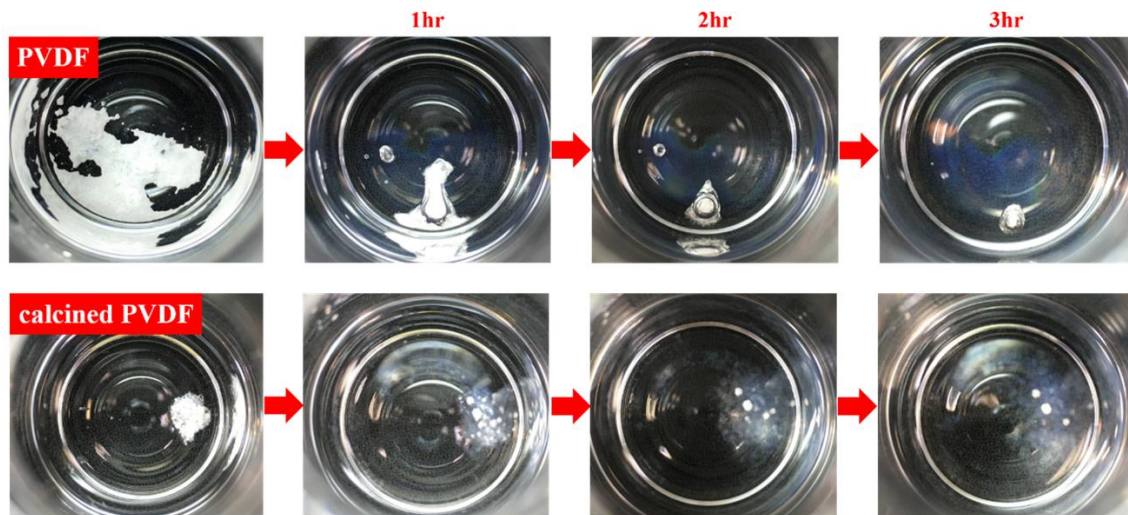
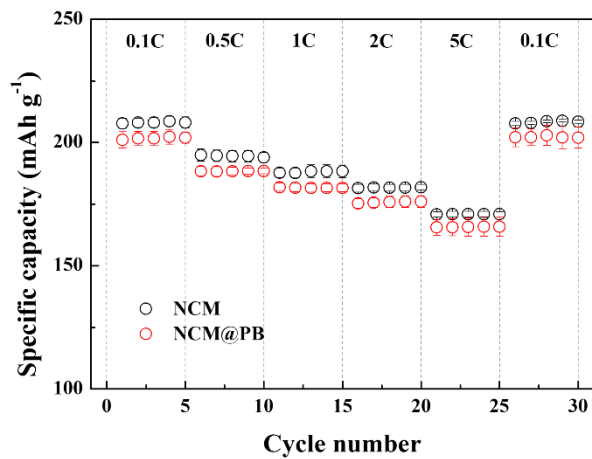
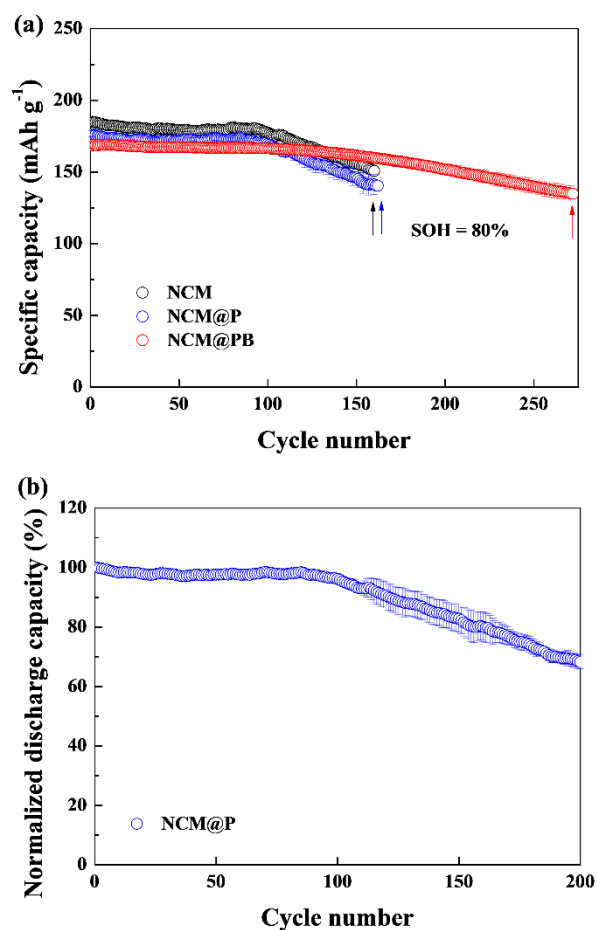


Figure S4. Solubility change of PVDF and 320°C calcined PVDF in NMP.



**Figure S5.** Rate capability of pristine NCM and NCM@PB (2.5-4.3V, error bars: standard deviation of three cells).



**Figure S6.** (a) Cycling performance of pristine NCM, NCM@P, NCM@PB at 1C-rate (2.5-4.3V; error bars: standard deviation of three cells) under room temperature; (b) Normalized cycling performance of NCM@P.

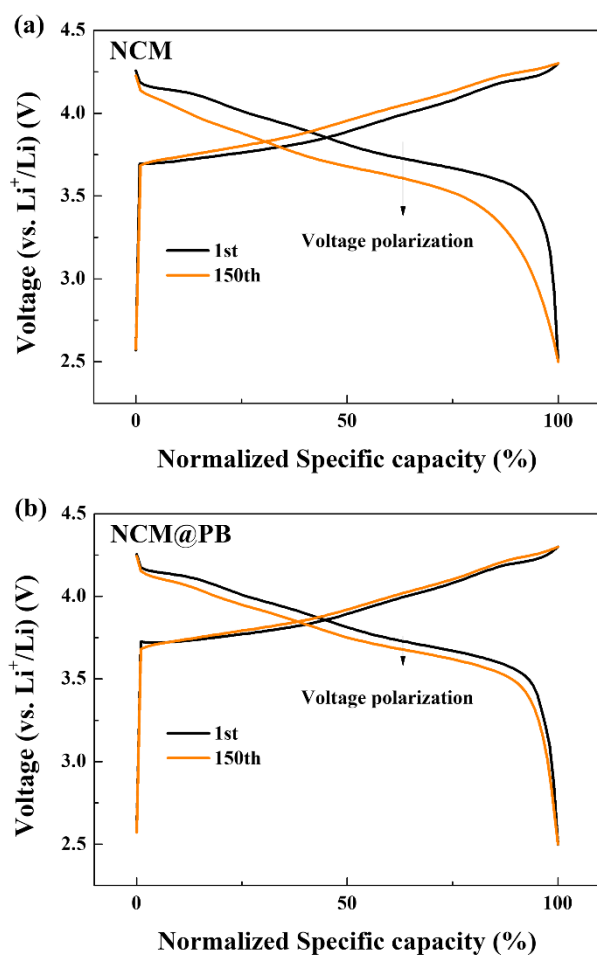


**Figure S7.** Normalized 1C-rate voltage profiles at different cycles of (a) pristine NCM and (b) NCM@PB.

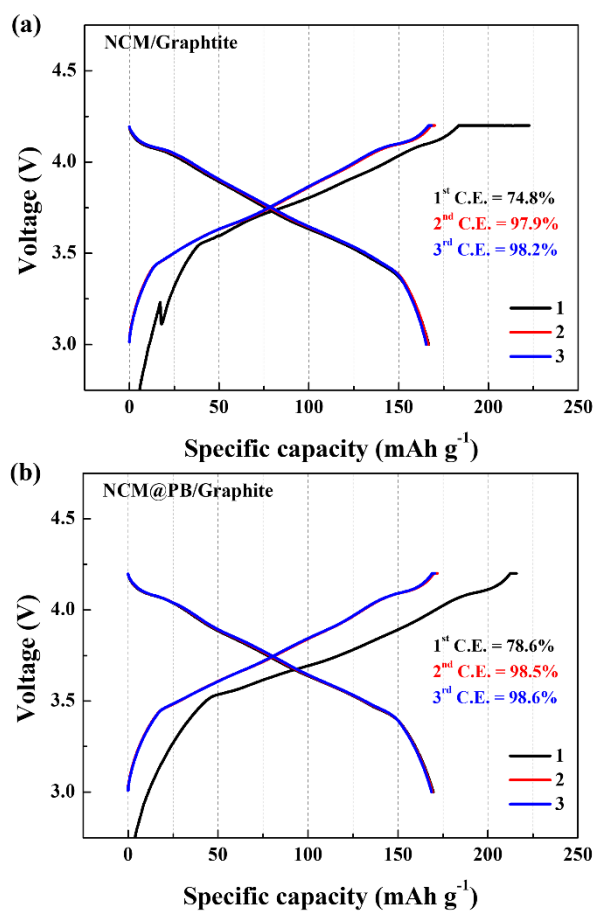


**Figure S8.** Formation cycles of (a) NCM/Graphite and (b) NCM@PB/Graphite full cells at 0.1C-rate.

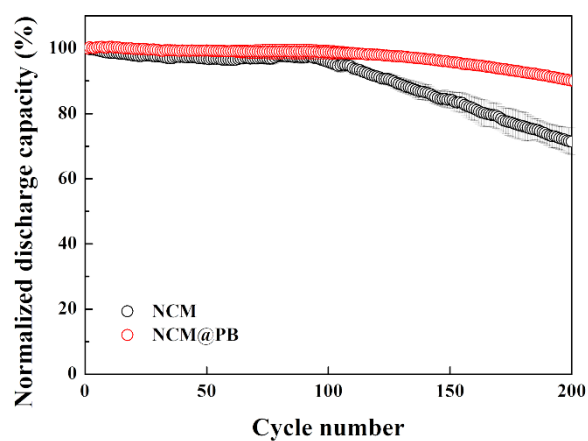


**Figure S9.** Normalized cycling performance of pristine NCM and NCM@PB at 1C-rate (2.5-4.3V; error bars: standard deviation of three cells).

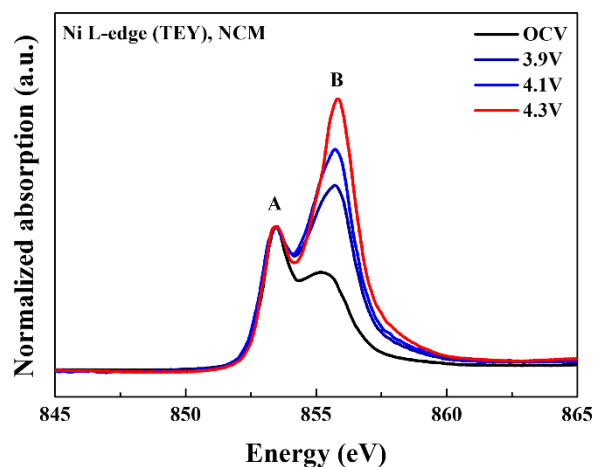


**Figure S10.** Ex situ Ni L<sub>3</sub>-edge spectra of pristine NCM during charging of the 1<sup>st</sup> cycle.

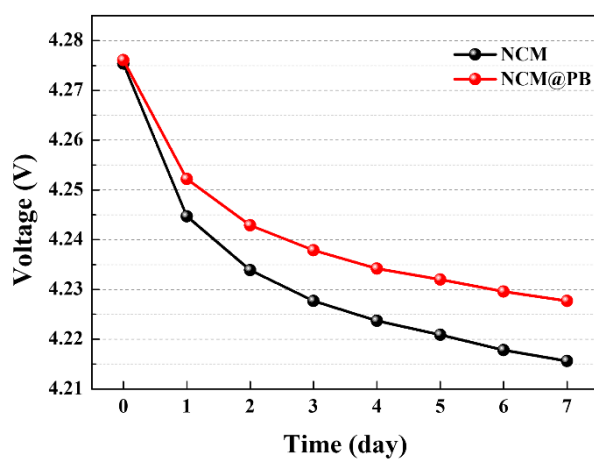


**Figure S11.** Self-discharge curves of pristine NCM and NCM@PB. Both cells were first charged to 4.3V and rest for 1 week. The voltage of both cells was recorded while resting. Note that the initial voltage is lower than 4.3V due to depolarization effect.



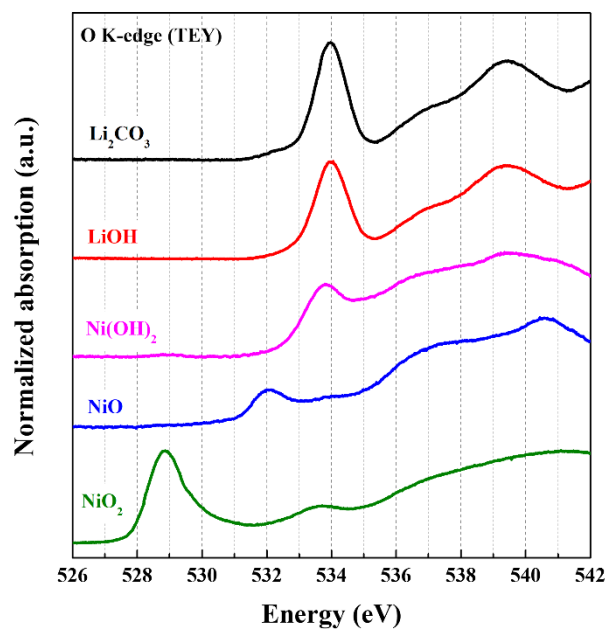


**Figure S12.** O K-edge spectra of  $\text{Li}_2\text{CO}_3$ ,  $\text{LiOH}$ ,  $\text{Ni}(\text{OH})_2$ ,  $\text{NiO}$  and  $\text{NiO}_2$ .

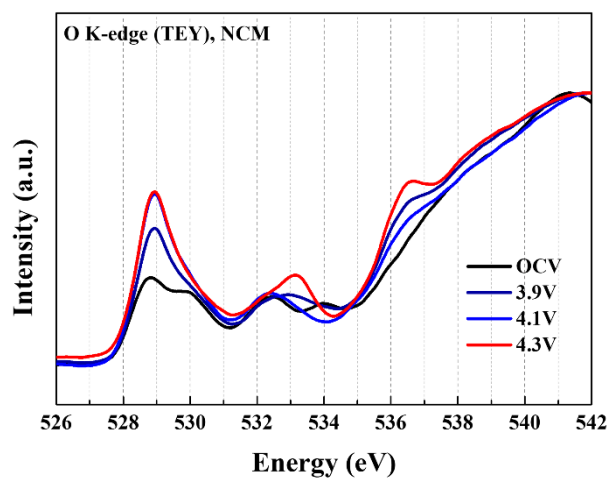


**Figure S13.** Ex situ O K-edge spectra of pristine NCM during charging of the 1<sup>st</sup> cycle.

**Table S3.** Summary of modification on Ni-rich cathodes

Surface modification material	Method	Cathode	Process temperature (time)	Voltage range (V v.s. Li <sup>+</sup> /Li)	Cycle stability (25 °C)	Thermal stability	Full cell performance	Ref.
Zr <sup>4+</sup>	Doping	LiNi <sub>0.83</sub> Co <sub>0.11</sub> Mn <sub>0.06</sub> O <sub>2</sub>	500 °C (6hr) → 830 °C (12hr)	3.0 – 4.3V	73.0%, 150 <sup>th</sup> at 1C	N.A.	N.A.	1
Al <sup>3+</sup>	Doping				74.7%, 150 <sup>th</sup> at 1C			
Zr <sup>4+</sup> /Al <sup>3+</sup>	Doping				89.7%, 150 <sup>th</sup> at 1C			
Mg <sup>2+</sup>	Doping		480 °C (5hr) → 750 °C (15hr)	2.8 – 4.3V	84.5%, 200 <sup>th</sup> at 2C	N.A.	N.A.	2
Li <sub>3</sub> PO <sub>4</sub>	Coating		480 °C (N.A.)		80.5%, 200 <sup>th</sup> at 2C			
Mg <sup>2+</sup> /Li <sub>3</sub> PO <sub>4</sub>	Doping +Coating		480 °C (5hr) → 750 °C (15hr) → 480 °C (N.A.)		90.0%, 200 <sup>th</sup> at 2C			
Nb <sup>5+</sup>	Doping		480 °C (5hr) → 750 °C (15hr)	2.8 – 4.3V	86.6%, 200 <sup>th</sup> at 1C	N.A.	N.A.	3
Mo <sup>6+</sup> /Li <sub>2</sub> MoO <sub>4</sub>	Doping +Coating		500 °C (12hr)	2.7 – 4.3V	90.22%, 100 <sup>th</sup> at 1C	N.A.	N.A.	4
W <sup>6+</sup>	Doping		80 °C (5hr) → 750 °C (15hr)	2.8 – 4.3V	69.9%, 500 <sup>th</sup> at 2C	N.A.	N.A.	5

Ti <sup>4+</sup> /LaNiLiO <sub>8</sub>	Doping +Coating	LiNi <sub>0.8</sub> Co <sub>0.1</sub> Mn <sub>0.1</sub> O <sub>2</sub>	480 °C (5hr) → 830 °C (12hr)	2.7 – 4.3V	90.55%, 200 <sup>th</sup> at 1C	15 °C-delayed decomp. temp. 43%-decreased heat release. 16%-decreased maximum heat flow.	N.A.	6
LiAlO <sub>2</sub>	Coating		480 °C (5hr) → 750 °C (15hr)	2.8 – 4.3V	85.8%, 200 <sup>th</sup> at 0.5C	11 °C-delayed decomp. temp. 47%-decreased heat release. 10%-decreased maximum heat flow.	N.A.	7
Li <sub>3</sub> PO <sub>4</sub> -AlPO <sub>4</sub> - Al(PO <sub>3</sub> ) <sub>3</sub>	Coating		600 °C (6hr)	3.0 – 4.3V	85.4%, 50 <sup>th</sup> at 0.5C	6 °C-delayed decomp. temp. 22%-decreased heat release. 24%-decreased maximum heat flow.	71.8%, 100 <sup>th</sup> at 0.5C	8
Li <sub>2</sub> MnO <sub>3</sub>	Coating		850 °C (5hr)	2.7 – 4.3V	80.4%, 500 <sup>th</sup> at 1C	14 °C-delayed decomp. temp. 45%-decreased heat release. 27%-decreased maximum heat flow.	N.A.	9
MgHPO <sub>4</sub>	Coating		500 °C (5hr) → 750 °C (15hr)	3.0 – 4.3V	86.3%, 100 <sup>th</sup> at 0.5C	N.A.	N.A.	10
<b>h-BN</b>	<b>Coating</b>	LiNi <sub>0.83</sub> Co <sub>0.12</sub> Mn <sub>0.05</sub> O <sub>2</sub>	<b>320 °C (0.5hr)</b>	<b>2.5 – 4.3V</b>	<b>92.0%, 200<sup>th</sup> at 1C</b>	<b>40 °C-delayed decomp. temp.</b> <b>44%-decreased heat release.</b> <b>41%-decreased maximum heat</b> <b>flow.</b>	<b>80%-capacity</b> <b>mark: 360<sup>th</sup></b> <b>cycle at 0.3C</b>	<b>This</b> <b>work</b>

## References

1. Z. Zhu, Y. Liang, H. Hu, A. Gao, T. Meng, D. Shu, F. Yi and J. Ling, *Journal of Power Sources*, 2021, **498**, 229857.
2. W. Xiao, Y. Nie, C. Miao, J. Wang, Y. Tan and M. Wen, *Journal of Colloid and Interface Science*, 2022, **607**, 1071-1082.
3. J. Wang, Z. Yi, C. Liu, M. He, C. Miao, J. Li, G. Xu and W. Xiao, *Journal of Colloid and Interface Science*, 2023, **635**, 295-304.
4. T. Teng, L. Xiao, L. Shen, J. Ran, G. Xiang, Y. Zhu and H. Chen, *Applied Surface Science*, 2022, **601**, 154101.
5. J. Wang, C. Liu, Q. Wang, G. Xu, C. Miao, M. Xu, C. Wang and W. Xiao, *Journal of Colloid and Interface Science*, 2022, **628**, 338-349.
6. H. P. Yang, H. H. Wu, M. Y. Ge, L. J. Li, Y. F. Yuan, Q. Yao, J. Chen, L. F. Xia, J. M. Zheng, Z. Y. Chen, J. Duan, K. Kisslinger, X. C. Zeng, W. K. Lee, Q. B. Zhang and J. Lu, *Advanced Functional Materials*, 2019, **29**.
7. W. Tang, Z. Chen, F. Xiong, F. Chen, C. Huang, Q. Gao, T. Wang, Z. Yang and W. Zhang, *Journal of Power Sources*, 2019, **412**, 246-254.
8. Z. Feng, R. Rajagopalan, D. Sun, Y. G. Tang and H. Y. Wang, *Chemical Engineering Journal*, 2020, **382**.
9. X. Huang, W. Zhu, J. Yao, L. Bu, X. Li, K. Tian, H. Lu, C. Quan, S. Xu, K. Xu, Z. Jiang, X. Zhang, L. Gao and J. Zhao, *Journal of Materials Chemistry A*, 2020, **8**, 17429-17441.
10. D.-Y. Hwang, H.-S. Kim and S.-H. Lee, *Journal of Materials Chemistry A*, 2022, **10**, 16555-16569.